AT&T Technical Journal
Vol. 64, No. 7, September 1985
Printed in U.S.A.

Thermal Buckling of Dual-Coated Fiber

By T. A. LENAHAN*

(Manuscript received August 8, 1984)

An analysis of buckling is presented for dual-coated fibers within their coating at low temperatures. Buckling causes microbending of the fiber axis, the prime source of added optical loss in the fiber. Buckling is caused by compressive stress exerted on the fiber by the coating, which arises because the thermal expansion coefficient of the coating is substantially larger than that of the fiber. Calculations show that buckling is more likely when the inner primary coating layer is soft and thick. Previous experimental results on fibers in cables indicate that softer, thicker primaries lead to more added loss at low temperatures, contrary to the simple model where lateral pressure imprints irregularities onto the path of the fiber. Such is the evidence that buckling occurs. The theory is applied to various coating designs. The calculated results rank the low-temperature performance reliably, but they also indicate that thermal strain falls short of the buckling strain. Other sources of strain are suggested, including a mechanism whereby irregularities induced by lateral pressure on the outside produce bending moments on the fiber.

I. INTRODUCTION

Optical fibers put in cables and/or subjected to low temperatures can have added transmission loss, attributed to microbending of the fiber axis.[1] Microbending can result from increased lateral pressure inside the cable, which imprints irregularities there onto the path of the fiber.[2] The imprinting is accentuated when the materials are stiffer, as at lower temperatures. Dual coatings (see Fig. 1) were introduced to reduce the effects of lateral pressure by buffering the fiber with a soft inner primary layer; the outer secondary layer is hard and robust

* AT&T Bell Laboratories.

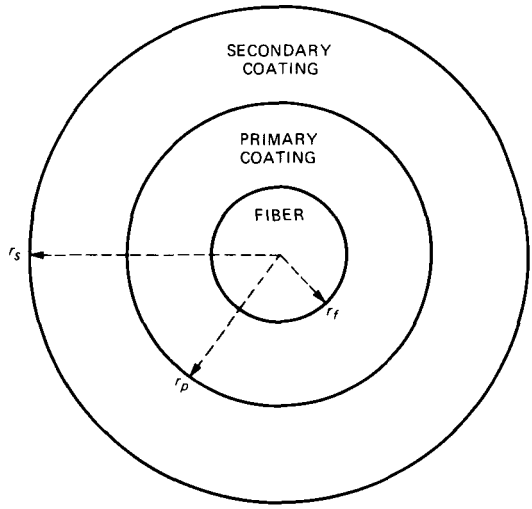

Fig. 1—A dual-coated fiber.

to allow handling. In practice, dual-coated fiber does indeed show substantially less added loss than single-coated fiber.[3]

Microbending also can arise from buckling of the fiber. Coating materials have thermal expansion coefficients two to three orders of magnitude larger than that of the fiber; hence, the coating exerts a compressive stress on the fiber at low temperatures. When the thermal strain exceeds a critical limit, the fiber buckles within the primary coating. Even below the buckling limit, thermal strain may amplify fiber bending already present. Buckling has been directly observed in (1) single-coated fiber within a soft elastomer under forced bending[4] and (2) dual-coated resistance wire under thermal stress.[5]

Indirect evidence exists for buckling of dual-coated fiber. Yabuta et al. report that thicker primary coatings lead to increased added loss at −50°C, irrespective of the outer secondary thickness, even though the primary material (silicone) remains soft at −50°C (see Fig. 7 of Ref. 6). This finding is not consistent with the simple lateral-pressure model, which says that more buffering gives less microbending. It is consistent with the buckling model because, as will be shown, thicker and softer primary layers provide less resistance to lateral displacement of the fiber and hence to fiber buckling. Results of the so-called S5 experiment,[7] involving various coating designs, likewise indicate that softer thicker primaries lead to more added loss at low temperatures.

In this paper thermal buckling of a dual-coated fiber within its coating is analyzed. Thermal strain on the fiber is calculated numerically and found to agree reasonably well with the simple rule of

mixtures. Buckling strain, the minimum strain required for the fiber to buckle, depends mainly on the lateral rigidity of the fiber in its coating and is measured by a spring constant κ, which is also calculated numerically. The buckling analysis of Refs. 5 and 6 was flawed because these references incorrectly assumed that κ was the modulus of the primary.

The theory is applied to various designs including ones of Yabuta and ones used in the S5 experiment. Results indicate, as above, that the fiber is more likely to buckle when the primary coating is soft and thick. The calculated thermal strain by itself is less than the calculated buckling strain in all cases, but other sources of strain can combine with the thermal to reach the buckling strain. For instance, thermal stress combined with irregularities in the secondary caused by lateral pressure would put moments on the fiber.

Whatever the exact mechanism for microbending, coating designs should account for the possibility of buckling. Experimental results indicate that the primary should be sufficiently thin, especially if the primary material remains soft at low temperatures.

In the next section the buckling analysis is developed and the associated numerical calculations are indicated. In Section III the theory is applied to the resistance wire of Katsuyama et al.[5] and other silicone/nylon coatings of Yabuta et al.[6] and designs from the S5 experiment.[7] The paper is summarized in Section IV and certain aspects outside the model that favor buckling are discussed. One of the most important aspects, already mentioned, is the prospect that irregular lateral pressure in conjunction with thermal stress produces bending moments on the fiber.

II. ANALYSIS

The analysis of fiber buckling involves the force or strain needed to buckle the fiber and the force actually on the fiber. In this section, after the mechanical properties of the relevant materials are indicated, the thermal strain of the fiber is calculated, and then the buckling strain is calculated. The fiber and coating are assumed throughout to be perfectly circular and concentric, homogeneous, and uniform along their length.

2.1 Materials characterization

Two kinds of structures are considered: dual-coated optical fiber and the dual-coated wire of Katsuyama. The dual-coated optical fibers considered have outer secondaries that are either an ultraviolet (UV)-cured urethane acrylate material (Borden) or nylon. The Borden secondary has as its inner primary either UV-cured material supplied

Table I—Material parameters

Material	E_g (psi)	$T = -40°C$ E (psi)	ν	$T = 0°C$ E (psi)	ν	α (°C^{-1})
Glass	1.07*E*7	1.07*E*7	0.25	1.07*E*7	0.25	5.04*E* − 7
Wire	2.35*E*7	2.35*E*7	0.25	2.35*E*7	0.25	1.6*E* − 5
Desolite	4.60*E*5	9.15*E*3	0.495	2.47*E*2	0.49987	1.2*E* − 4
Hot Melt	—	3.34*E*2	0.49982	9.15*E*1	0.49995	1.4*E* − 4
Silicone	—	2.64*E*2	0.49986	1.47*E*2	0.49992	3.0*E* − 4
Borden	6.48*E*5	5.15*E*5	0.30	1.96*E*5	0.4244	0.6*E* − 4
Nylon	—	3.08*E*5	0.333	2.93*E*5	0.341	1.0*E* − 4

by De Soto (Desolite*) or a thermoplastic material (Hot Melt). The nylon secondary has silicone as its primary material; this combination is used for the wire of Katsuyama et al.[5] and for optical fiber studied by Yabuta et al.[6]

The modulus E, Poisson ratio ν, and thermal expansion coefficient α are the mechanical properties needed in the buckling analysis. The glass fiber and wire are elastic in the temperature range of interest; hence, a single value for the mechanical parameters characterizes these materials. The coatings are viscoelastic polymeric materials; their modulus values relax over time and depend on temperature. We simplify the modulus values here by considering only their values at 24 hours (a typical time span for temperature drops from room temperature to −40°C).

The values of E and α for the fiber are taken from Table III of Ref. 8 and for the wire from Ref. 5. Their Poisson ratio is taken as $\nu = 0.25$, the accepted value for a material in its glassy (stiff) state. These values appear in Table I.

The 24-hour modulus E of Desolite, Hot Melt, and Borden are shown as functions of temperature in Figs. 2 through 4, respectively. These moduli were synthesized from oscillatory data from a rheometric thermal mechanical spectrometer. Modulus values for 0 and −40°C appear in Table I. The thermal expansion coefficients (at low temperatures) of Desolite and Hot Melt and Borden have been taken from Refs. 9 and 8, respectively. Values of E at 0 and −40°C for silicone and nylon are taken from Ref. 5; the value of α for silicone comes from Ref. 10 and for nylon from Ref. 6. These all appear in Table I.

The Poisson ratios of the coating materials are estimated by assuming that the bulk modulus,

$$K = \frac{E}{3(1 - 2\nu)}, \tag{1}$$

* Registered trademark of De Soto, Inc.

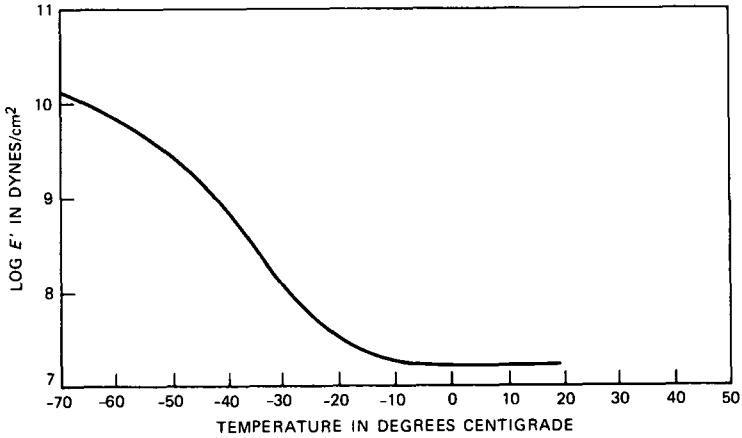

Fig. 2—Isochronal plot (24 hours) for the Young's modulus of Desolite versus temperature.

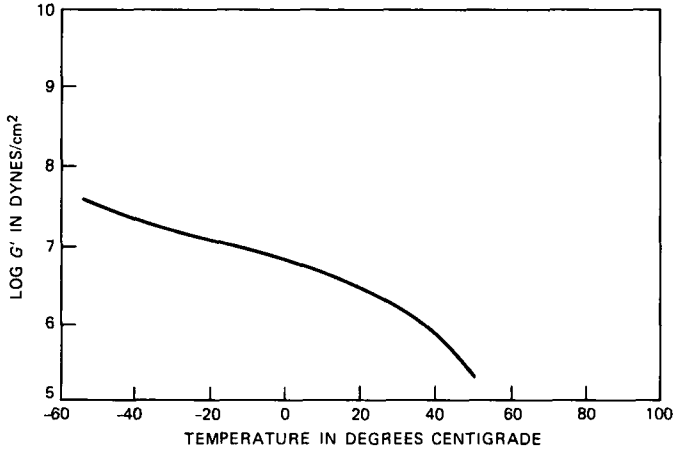

Fig. 3—Isochronal plot (24 hours) for the shear modulus of Hot Melt versus temperature.

is independent of temperature. Studies[11] have shown that K increases only by about a factor of 2 (though E increases several decades) as the material goes from a rubbery to a glassy state. Taking $\nu = 0.25$ at the low temperature glassy plateau (where $E = E_g$), ν is determined at any temperature by

$$\nu = 0.50 - 0.25E/E_g, \tag{2}$$

derived from the constancy of K.

The values of E_g are taken from the 1- or 2-second modulus at the lowest temperature measured (typically −60°C). For primary materials

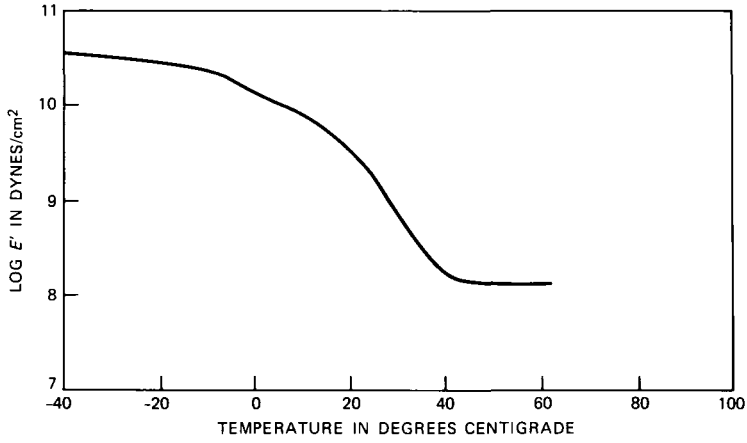

Fig. 4—Isochronal plot (24 hours) for the Young's modulus of Borden versus temperature.

where a plateau value was not attained or was unavailable, the E_g for Desolite was used to estimate ν. Available values of E_g and calculated values of ν appear in Table I.

2.2 Thermal strain

The different thermal expansion coefficients can be consolidated into an effective expansion coefficient α_{eff} for the coated fiber (or wire) as a whole. The rule of mixtures[8] approximates α_{eff} by weighting the various expansion coefficients by the cross-sectional area and the modulus of the corresponding materials. For N materials the formula is

$$\alpha_{\text{eff}} = \sum_{n=1}^{N} \alpha_n A_n E_n \Big/ \sum_{n=1}^{N} A_n E_n, \tag{3}$$

where α_n denotes the expansion coefficient, A_n the area, and E_n the modulus of the nth material.

The rule of mixtures is exact when the coupling of radial displacements is neglected, as if the fiber and coating layers were parallel springs joined at the ends. An analysis accounting for radial coupling is described in Appendix A. Deviations from the rule of mixtures are usually within a few percent, but examples have been found with deviations from −15 to +36 percent.

The thermal strain of the fiber for a temperature change T_0 to T_1 is

$$\epsilon_{\text{therm}} = \int_{T_0}^{T_1} (\alpha_{\text{eff}} - \alpha_{\text{fib}}) dT, \tag{4}$$

where α_{fib} denotes the thermal expansion coefficient of the fiber by

itself. In general, α_{eff} will depend on time and temperature through its dependence on E and α of the coating materials. With this information, the strain of the fiber can be determined as a function of time for any temperature cycling as in Ref. 8.

For simplicity, the α_{eff} will be taken here as the effective expansion coefficient averaged over the range of temperature change. As for α_{fib}, it is independent of temperature; so the thermal strain of the fiber for a temperature change T is simply

$$\epsilon_{\text{therm}} = (\alpha_{\text{eff}} - \alpha_{\text{fib}})T. \tag{5}$$

The value of α_{eff} will be estimated by using 24-hour modulus values at −40°C and, for comparison, 0°C.

2.3 Buckling analysis

The fiber (or wire) may buckle and follow a wavelike path because of compressive strain. The theory of elastic stability[12] is used to study the buckling of fibers within their coating.

The fiber is treated as a beam in an elastic medium. A force and moment balance yields the differential equation

$$E_f I \frac{d^4y}{dz^4} + F \frac{d^2y}{dz^2} + \kappa y = 0 \tag{6}$$

for the deflection y of the fiber as a function of the distance z along the fiber. Small deflections are assumed. The parameters E_f, I, and F denote the modulus of the fiber, the moment of inertia of the fiber ($\pi r_f^4/4$ for radius r_f), and the compressive force on the fiber, respectively. The parameter κ denotes the spring constant of the fiber, which is the ratio of the centering force exerted by the coating to the displacement of the fiber from center.

Early work incorrectly assumed that $\kappa = E_p$,[5,6] but Vangheluwe,[13] assuming a rigid secondary, determined that

$$\kappa = \frac{4\pi E_p(1 - \nu_p)(3 - 4\nu_p)}{(1 + \nu_p)\left[(3 - 4\nu_p)^2 \ln(r_p/r_f) - \dfrac{(r_p/r_f)^2 - 1}{(r_p/r_f)^2 + 1}\right]}, \tag{7}$$

where subscript p signifies the primary region and f the fiber (or wire). A numerical calculation of κ, which accounts for the elasticity of the secondary, is described in Appendix B. The two calculations give identical results when the secondary is assumed rigid. Results indicate that the elasticity of the secondary can reduce κ by more than 80 percent.

The buckling solution has the form

$$y = A \sin\left(\frac{2\pi z}{P}\right), \tag{8}$$

where A is an arbitrary amplitude and P is the pitch. (This form in conjunction with

$$x = A \cos\left(\frac{2\pi z}{P}\right) \tag{9}$$

for the orthogonal component covers the case of helical buckling.) Substituting y into eq. (6) gives

$$A\left[E_f I\left(\frac{2\pi}{P}\right)^4 - F\left(\frac{2\pi}{P}\right)^2 + \kappa\right] \sin\left(\frac{2\pi z}{P}\right) = 0. \tag{10}$$

Hence, the force required for the fiber to buckle with pitch P is

$$F = E_f I\left(\frac{2\pi}{P}\right)^2 + \kappa\left(\frac{P}{2\pi}\right)^2. \tag{11}$$

The minimum buckling force is

$$F_{\min} = 2\sqrt{E_f I \kappa} = r_f^2 \sqrt{\pi E_f \kappa}, \tag{12}$$

corresponding to a pitch of

$$P_{\min} = 2\pi(E_f I/\kappa)^{1/4} = \pi r_f (4\pi E_f/\kappa)^{1/4}. \tag{13}$$

The corresponding strain of the fiber is

$$\epsilon_{\min} = F_{\min}/\pi r_f^2 E_f = \sqrt{\frac{\kappa}{\pi E_f}}. \tag{14}$$

This formula shows that fibers having smaller spring constants, which are associated with softer and/or thicker primaries, require less strain to buckle.

If $\epsilon_{\text{therm}} > \epsilon_{\min}$, then the fiber will buckle in its coating. If $\epsilon_{\text{therm}} < \epsilon_{\min}$, then buckling can still occur if $\epsilon_{\text{therm}} + \epsilon_{\text{res}} > \epsilon_{\min}$, where ϵ_{res} denotes residual strain caused by initial bending or other moments. Even if $\epsilon_{\text{therm}} + \epsilon_{\text{res}} < \epsilon_{\min}$, thermal bending can occur. In thermal bending, initial bending or other moments of the fiber are accentuated by the thermal stress. The size of the effect grows as $(\epsilon_{\min} - \epsilon_{\text{therm}} - \epsilon_{\text{res}})^{-1}$, as shown in Ref. 12.

III. APPLICATIONS

In this section the buckling analysis is applied to the dual-coated wire of Katsuyama, for which buckling was observed, and to various dual-coated fiber designs. Parameter studies are also presented.

3.1 Wire of Katsuyama and fibers of Yabuta

The wire of Katsuyama et al.[5] had a dual coating where the primary/secondary was composed of silicone/nylon. The material parameters

for these are given in Table I. The wire radius was $r_w = 75$ μm. The outer radii of the primary (r_p) and the secondary (r_s) were $r_p/r_s = 175$ μm/600 μm.

The calculated spring constant is $\kappa = 6.9E3$ psi, and effective thermal expansion coefficient is $\alpha_{\text{eff}} = 5.37E - 5$°C. If we assume a temperature drop of 100°C, the strain on the wire from eq. (5) is $\epsilon_{\text{therm}} = 0.38$ percent, and the minimum buckling strain from eq. (14) is $\epsilon_{\text{min}} = 0.97$ percent with a pitch of $P_{\text{min}} = 3.39$ mm. These values were obtained using the material parameters for −40°C. For 0°C, where the coating materials are somewhat softer, the calculations give $\kappa = 3.87E3$ psi and $\alpha_{\text{eff}} = 5.25E - 5°\text{C}^{-1}$; the same temperature change of 100°C gives $\epsilon_{\text{therm}} = 0.37$ percent and $\epsilon_{\text{min}} = 0.72$ percent with a pitch of 3.92 mm. These calculated values are summarized in Table II.

As buckling did occur in the Katsuyama wire at −70°C, the difference $\epsilon_{\text{min}} - \epsilon_{\text{therm}}$ estimates the residual strain ϵ_{res} in the wire at 30°C. Relative to the −40°C parameters, $\epsilon_{\text{res}} \sim 0.59$ percent; relative to the 0°C parameters, $\epsilon_{\text{res}} \sim 0.35$ percent.

Yabuta et al. (see Fig. 7 of Ref. 6) studied the silicone/nylon coating system on optical fibers. One design having a relatively thick primary had substantial added loss at −50°C; its dimensions were $r_p/r_s = 250$ μm/471 μm. Another design with a thinner primary had negligible added loss even though the secondary had somewhat more cross-sectional area; its dimensions were 100 μm/448 μm. The fiber radius for both was $r_f = 62.5$ μm.

Calculated values for κ, α_{eff}, ϵ_{therm}, ϵ_{min}, and P_{min} are given in Table II for both designs using both 0 and −40°C material parameters from Table I. For the lower-temperature parameters, the thick primary gives $\epsilon_{\text{therm}} = 0.61$ percent and $\epsilon_{\text{min}} = 0.81$ percent with a pitch of 3.09 mm, and the thin primary gives $\epsilon_{\text{therm}} = 0.59$ percent and $\epsilon_{\text{min}} = 3.10$ percent with a pitch of 1.57 mm. These values indicate that buckling

Table II—Buckling quantities for certain silicone coatings

Temp.	κ (psi)	α_{eff} (°C^{-1})	ϵ_{therm} (%)	ϵ_{min} (%)	P_{min} (mm)
		(a) Katsuyama et al.			
−40°C	6899	$5.367E - 5$	0.377	0.967	3.39
0°	3868	$5.253E - 5$	0.365	0.724	3.92
		(b) Yabuta et al., poor			
−40°C	2184	$6.146E - 5$	0.610	0.806	3.09
0°	1219	$5.969E - 5$	0.592	0.602	3.57
		(c) Yabuta et al., good			
−40°C	32393	$5.898E - 5$	0.585	3.104	1.57
0°	18571	$5.772E - 5$	0.572	2.350	1.80

in the first case is at least as probable as for the Katsuyama wire, but much less probable in the second.

3.2 S5 experiment

Four dual-coat designs were selected from the S5 experiment.[7] Their performance, based on added loss at low temperatures, ranged from good to bad. Figure 5 shows the added loss versus temperature for the best and worst cases.

Three of the four designs used UV-cured Desolite for the primary, the other used Hot Melt. All used Borden for the secondary. The coating dimensions varied in primary outer diameter/secondary outer diameter from 8/13 to 11/15, expressed in mils. The designs are

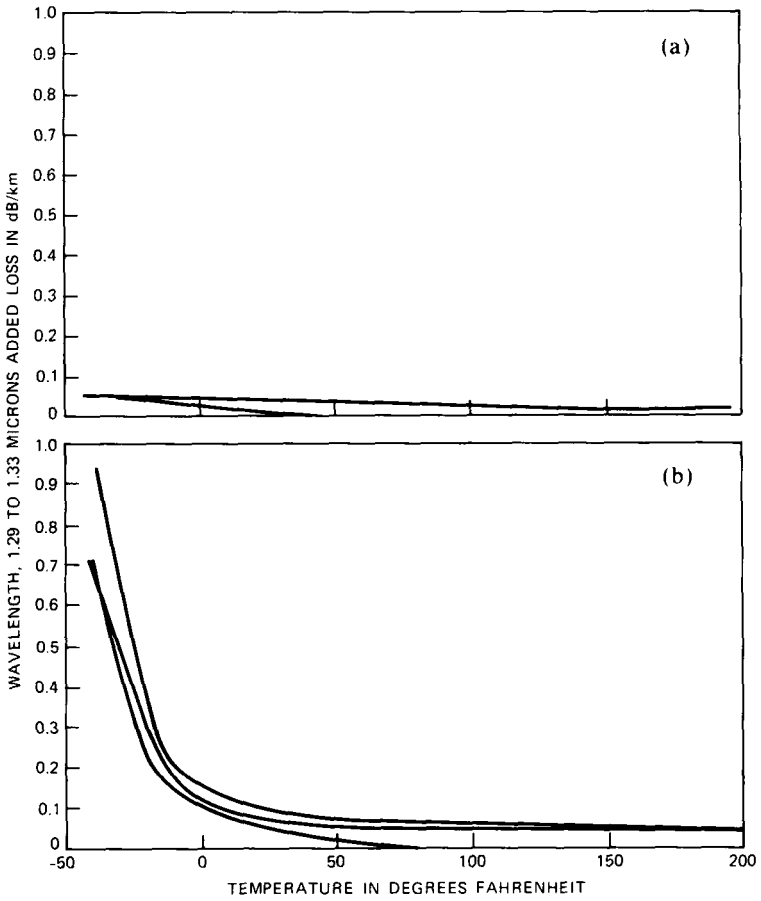

Fig. 5—Added loss at $\lambda \sim 1.3$ μm versus temperature for the (a) best coatings from the S5 experiment and (b) worst coatings from the S5 experiment.

Table III—S5 experiment

Size (mils)	Temp. (°C)	Coat (P)	Rank	κ (kpsi)	α_{eff} ($°C^{-1}$)	ϵ_{therm} (%)	ϵ_{min} (%)	P_{min} (mm)
8/13	−40	UV	Best	570.6	$0.112E-4$	0.107	13.03	0.76
	0			28.6	$0.487E-5$	0.044	2.92	1.61
10/13	−40	UV	Second	288.8	$0.855E-5$	0.081	9.27	0.90
	0			10.3	$0.349E-5$	0.030	1.75	2.07
11/15	−40	UV	Third	218.1	$0.120E-4$	0.115	8.05	0.97
	0			7.47	$0.494E-5$	0.044	1.49	2.18
11/15	−40	Hot Melt	Worst	10.1	$0.138E-4$	0.133	1.73	2.08
	0			2.78	$0.511E-5$	0.046	0.91	2.88

specified in Table III, together with calculated values of κ, α_{eff}, ϵ_{therm} (for a 100°C temperature drop), and ϵ_{min} and P_{min} using the material parameters for −40 and 0°C.

The calculated difference $\epsilon_{\text{min}} - \epsilon_{\text{therm}}$ tracks the performance rank of the design for both 0 and −40°C. The design with the stiffest and thinnest primary had the least added loss; the one with the softest, thickest primary had the most.

3.3 Parameter studies

The thermal and buckling strains depend on the geometry and materials of the coating. This dependence is now studied in general terms.

The thermal strain ϵ_{therm} is proportional to the quantity, $\alpha_{\text{eff}} - \alpha_{\text{fib}}$. By the rule of mixtures,

$$\alpha_{\text{eff}} - \alpha_{\text{fib}} = \frac{A_p E_p(\alpha_p - \alpha_{\text{fib}}) + A_s E_s(\alpha_s - \alpha_{\text{fib}})}{A_f E_f + A_p E_p + A_s E_s}. \tag{15}$$

Usually, both the area A_p and modulus E_p of the primary are much smaller than A_s and E_s of the secondary. Neglecting terms with $A_p E_p$ gives

$$\alpha_{\text{eff}} - \alpha_{\text{fib}} \simeq \frac{A_s E_s(\alpha_s - \alpha_{\text{fib}})}{A_f E_f + A_s E_s} = \frac{\alpha_s - \alpha_{\text{fib}}}{1 + (A_f E_f / A_s E_s)} \tag{16}$$

or

$$\alpha_{\text{eff}} - \alpha_{\text{fib}} \simeq (\alpha_s - \alpha_{\text{fib}}) \Big/ \left[1 + \frac{E_f/E_s}{(r_s/r_f)^2 - (r_p/r_f)^2}\right]. \tag{17}$$

Figure 6 shows plots of this expression versus r_s/r_f, assuming $E_f/E_s = 20$ (as for Borden at −40°C) and $E_f/E_s = 50$ (as for Borden at 0°C) and also $r_p/r_f = 1.5$. The plots again show the well-known fact that larger, stiffer secondaries produce more thermal strain than smaller, softer ones.

The buckling strain ϵ_{min} from eq. (14) is proportional to $\sqrt{\kappa}$ and inversely proportional to $\sqrt{E_f}$. The latter implies that wire filaments,

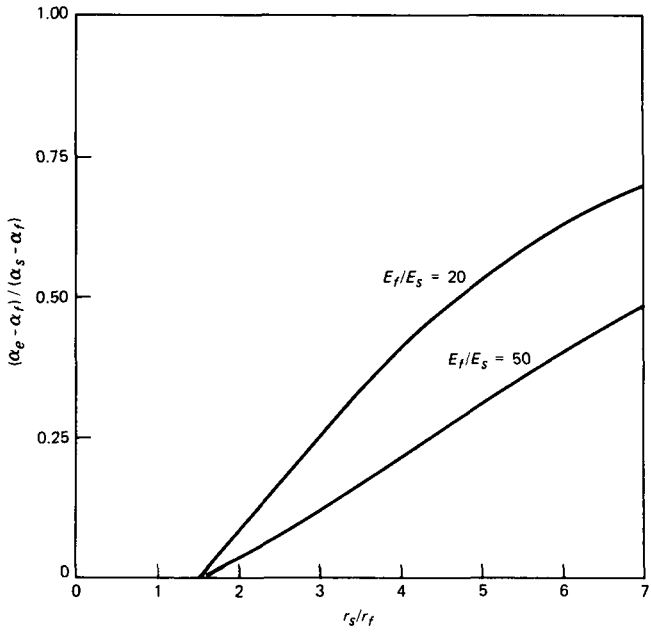

Fig. 6—Effective thermal expansion coefficient versus secondary radius for two secondary modulus values according to the rule of mixtures.

having a higher modulus, require less strain to buckle than glass fibers. The spring constant κ will be studied first for a rigid secondary to which the formula of Vangheluwe in eq. (7) applies. The elasticity of the secondary will be considered subsequently.

If $X \equiv r_p/r_f$ is close to 1, the approximation[14]

$$\ln X \simeq \frac{X^2 - 1}{X^2 + 1} + \frac{1}{3}\left(\frac{X^2 - 1}{X^2 + 1}\right)^3 \tag{18}$$

gives (for $\nu = \nu_p$)

$$\kappa \simeq \frac{4\pi E_p(1 - \nu)(3 - 4\nu)}{(1 + \nu)\left[8(1 - \nu)(1 - 2\nu)\dfrac{X^2 - 1}{X^2 + 1} + \dfrac{(3 - 4\nu)^2}{3}\left(\dfrac{X^2 - 1}{X^2 + 1}\right)^3\right]}. \tag{19}$$

When $\nu \simeq 1/2$, eq. (19) reduces to

$$\kappa \simeq \frac{4\pi E_p(X^2 + 1)^3}{(X^2 - 1)^3}; \tag{20}$$

when ν is not close to 1/2 and $X \simeq 1$, eq. (19) reduces to

$$\kappa \simeq \frac{\pi E_p}{2(1 - 2\nu)}\left(\frac{3 - 4\nu}{1 + \nu}\right)\frac{X^2 + 1}{X^2 - 1} = \frac{\pi K_p}{G}\left(\frac{3 - 4\nu}{1 + \nu}\right)\frac{X^2 + 1}{X^2 - 1}, \tag{21}$$

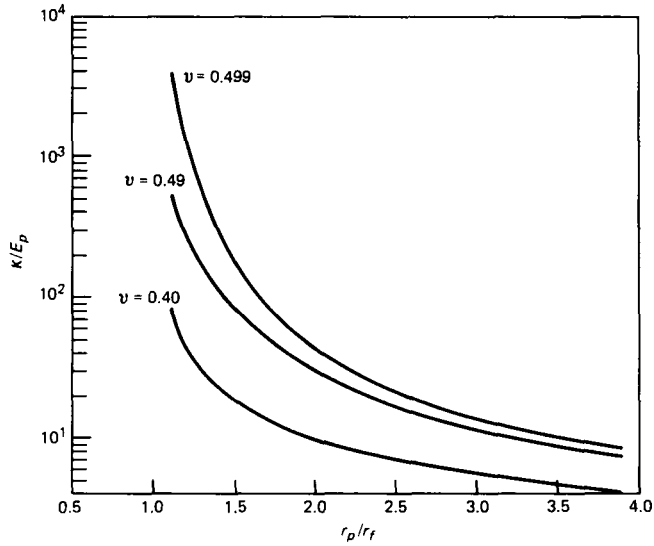

Fig. 7—Spring constant versus primary radius for three Poisson ratios assuming a rigid secondary.

where K_p denotes the bulk modulus of the primary. In all cases, κ increases without bound as X approaches 1 (i.e., as the primary becomes thinner). If X is large, the logarithmic term in the denominator dominates to give

$$\kappa = \frac{4\pi E_p(1 - \nu)}{(1 + \nu)(3 - 4\nu)\ln r_p/r_f}. \tag{22}$$

Thus, κ goes to 0 as r_p/r_f becomes large.

Figure 7 shows κ/E_p plotted versus r_p/r_f for $\nu = 0.40$, 0.49, and 0.499. The curves illustrate the asymptotic behavior of κ given above. They also indicate that thicker primaries have smaller κ with greatest sensitivity when ν is close to 1/2. The compliance of the secondary leads to lower κ.

Figure 8 shows κ versus r_s/r_f for $E_s = 500$, 200, and 100 kpsi with corresponding $\nu_s = 0.3$, 0.42, and 0.46, respectively (chosen to keep the bulk modulus fixed). The primary was assumed to be Desolite at −40°C with $r_p/r_f = 1.5$. The curves show that κ is smaller for thicker, more compliant secondaries. The compliance of the secondary can cause κ to drop to 20 percent of the value from the formula of Vangheluwe.

IV. SUMMARY AND CONCLUSIONS

This paper has concerned buckling of dual-coated optical fiber caused by compressive stress on the fiber exerted by the coating at

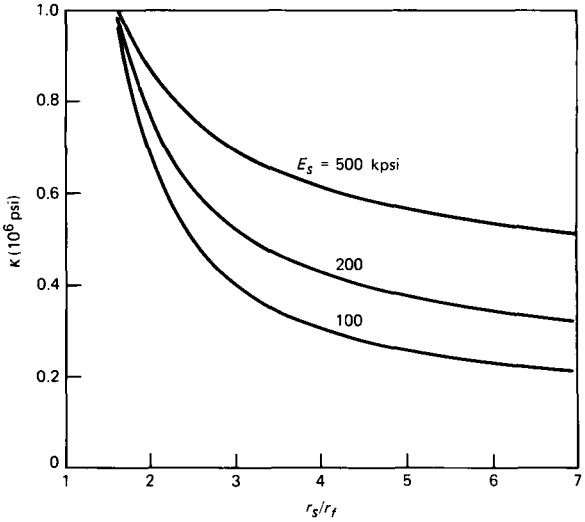

Fig. 8—Spring constant versus secondary radius for three Poisson ratios of the secondary assuming a Desolite primary at −40°C with $r_p/r_f = 1.5$.

low temperatures. The stress arises because the thermal expansion coefficient of the coating is substantially larger than that of the fiber.

Buckling is one of two mechanisms used to explain microbending of the fiber axis, the prime source of added optical loss in the fiber. In the other method, lateral pressure imprints irregularities around the fiber onto the path of the fiber. This occurs at room, as well as low, temperatures and in single-coated, as well as dual-coated, fiber. The antidote to lateral pressure is dual coating where the inside primary coating buffers the fiber and decouples it from the outside. However, too much buffering has been found to produce more added loss at low temperatures, presumably due to buckling.

Two basic ways exist for preventing buckling. The thermal strain on the fiber might be decreased, or the strain needed to buckle might be increased.

Thermal strain depends mostly on the secondary layer. Smaller secondaries put less strain on the fiber; secondaries of a more compliant material or ones with a smaller thermal expansion coefficient have the same effect. These changes are compatible with the dictates of the simple lateral-pressure model.

The buckling strain depends on the spring constant κ. Thinner primaries and, to a lesser extent, thinner secondaries have larger buckling strains. Stiffer primary materials and, to a lesser extent, stiffer secondary materials provide the same effect. The magnitude of these effects is indicated in Fig. 7 for the primary and in Fig. 8 for the secondary. In general, reduced buffering provides more resistance to

buckling—just the opposite of what the simple lateral-pressure model dictates.

Experimental results indicate that buckling does occur. In the silicone/nylon coatings of Yabuta et al.,[6] thicker primaries were associated with substantially more added loss at low temperatures. Calculations in Section III showed that the coating with thin primary and low added loss at −40°C needs about four times as much strain to buckle as the one with thick primary and high added loss at −40°C. The primary material (silicone) remains relatively compliant (264 psi) at this temperature. The experimental results are consistent with the buckling mechanism, but not with the lateral pressure mechanism by itself. Similar results were found for fibers in the S5 experiment.[7] Thick primaries of the compliant Hot Melt material performed poorly compared with thinner primaries of De Soto, which stiffens at low temperatures. This outcome may be explained by the buckling calculations in Section III, which indicate that the spring constant for the latter coating is 50 times greater than for the former.

Nevertheless, the calculated thermal strain was less than the buckling strain in all cases, even for the wire of Katsuyama et al. where buckling was known to have occurred. The short fall may be explained by various factors outside the model, as follows:

1. Initial bending (e.g., stranding) involves a strain on the fiber, which adds to the thermal strain to bring the total closer to the buckling strain.

2. The thermal strain depends on the temperature drop, which was taken as 100°C. The precise temperature drop should be measured from a reference temperature where the residual stress on the fiber is 0. Because this temperature is uncertain, the temperature drop is also and might be more than 100°C.

3. Asymmetry of the coating or eccentricity of the fiber in its coating in conjunction with thermal stress produces bending moments along the fiber because, at equilibrium, moments on the coating must be balanced by moments on the fiber. These deformations can arise from imperfections in the coating process or lateral pressure in the cable. Thus, irregularities associated with lateral pressure can be transmitted to the fiber despite the buffering protection by the primary layer.

4. Thermal bending, a precursor to buckling, would produce a steadily increasing added optical loss as temperature drops for strains below the buckling strain.

Other omissions include details of the viscoelastic nature of the coating materials, the thermal dependence of the expansion coefficients, the thermal cycling, and thermal gradients. The buckling calculations must be regarded as estimates most valuable in making comparisons.

V. ACKNOWLEDGMENTS

The author thanks C. J. Aloisio for initially describing the buckling problem and continued discussion, C. R. Taylor for modulus measurements and continued discussion, C. H. Gartside III for discussion of the S5 experiment, L. L. Blyler, Jr., for measurements of thermal expansion coefficients, and D. P. Woodard and J. T. Loadholt for discussions.

REFERENCES

1. W. B. Gardner, "Miocrobending Loss in Optical Fibers," B.S.T.J., *54*, No. 2 (February 1975), pp. 457–65.
2. D. Gloge, "Optical-Fiber Packaging and Its Influence on Fiber Straightness and Loss," B.S.T.J., *54*, No. 2 (February 1975), pp. 245–62.
3. L. L. Blyler et al., "A New Dual-Coating System for Optical Fibers," Eighth European Conf. Opt. Commun., Cannes, France, 1982.
4. L. L. Blyler, Jr., et al., "Buckling of Optical Fibers Within Elastomers Used in an Embedded-Core Cable Structure," Int. Wire Cable Symp. Proc. 1983, pp. 144–50.
5. Y. Katsuyama et al., "Transmission Loss of Coated Single-Mode Fiber at Low Temperatures," Appl. Opt., *19*, No. 24 (December 15, 1980), pp. 4200–5.
6. T. Yabuta et al., "Excess Loss of Single-Mode Jacketed Optical Fiber at Low Temperature," Appl. Opt., *22*, No. 15 (August 1, 1983), pp. 2356–62.
7. C. H. Gartside, unpublished work.
8. G. S. Brockway and M. R. Santana, "Analysis of Thermally Induced Loss in Fiber-Optic Ribbons," B.S.T.J., *62*, No. 4, Part 1 (April 1983), pp. 993–1018.
9. L. L. Blyler, Jr., unpublished work.
10. C. R. Taylor, private communication.
11. J. D. Ferry, *Viscoelastic Properties of Polymers*, Second Edition, New York: Wiley, 1970.
12. S. P. Timoshenko, *Theory of Elastic Stability*, Second Edition, New York: McGraw-Hill, 1961.
13. D. C. L. Vangheluwe, "Exact Calculations of the Spring Constant in the Buckling of Optical Fibers," Appl. Opt., *23*, No. 13 (July 1, 1984), pp. 2045–6.
14. C. D. Hodgman, Editor, *C.R.C. Standard Mathematical Tables*, Twelfth Edition, Cleveland: Chemical Rubber Publishing Co., 1959, p. 373.
15. I. S. Sokolnikoff, *Mathematical Theory of Elasticity*, Second Edition, New York: McGraw-Hill, 1956.

APPENDIX A

Calculation of Thermal Stress

This appendix gives a method for calculating the effective expansion coefficient of a dual-coated fiber. The calculation goes beyond the rule of mixtures by treating the coupling of the radial displacements of the various layers.

Define cylindrical coordinates (r, θ, z) based at the center of the coated fiber. The displacement in each of the three regions can be represented by

$$U = \begin{pmatrix} U_r \\ U_\theta \\ U_z \end{pmatrix} = \begin{pmatrix} \frac{a_n}{r} + b_n r \\ 0 \\ Cz \end{pmatrix} n = 1, 2, 3. \tag{23}$$

The fiber has $n = 1$, the primary coating $n = 2$, and the secondary $n = 3$. This vector function satisfies the Cauchy Navier equation[15] for displacements and represents a solution without warping (because C is independent of n) or angular deformation.

The strain components are

$$\epsilon_{rr} = \frac{\partial U_r}{\partial r} = -\frac{a_n}{r^2} + b_n$$

$$\epsilon_{\theta\theta} = \frac{1}{r}\frac{\partial U_\theta}{\partial \theta} + \frac{U_r}{r} = \frac{a_n}{r^2} + b_n$$

$$\epsilon_{\theta\theta} = \frac{\partial U_z}{\partial z} = C$$

$$\epsilon_{\theta z} = \epsilon_{\theta r} = \epsilon_{rz} = 0. \tag{24}$$

The first invariant of the strain tensor is

$$e = \epsilon_{rr} + \epsilon_{\theta\theta} + \epsilon_{zz} = 2b_n + C. \tag{25}$$

Stress components are obtained from the generalized Hooke's law,

$$\sigma_{ij} = \lambda e \delta_{ij} + 2G\epsilon_{ij} - \beta T \delta_{ij}, \tag{26}$$

which gives

$$\sigma_{rr} = \lambda e + 2G\epsilon_{rr} - \beta T$$

$$\sigma_{zz} = \lambda e + 2G\epsilon_{zz} - \beta T, \tag{27}$$

where

$$\beta = \frac{E}{1 - 2\nu} \quad G = \frac{E}{2(1 + \nu)} \quad \lambda = \frac{2G\nu}{1 - 2\nu}, \tag{28}$$

α is the thermal expansion coefficient, and T is the temperature change. The material parameters are assumed to depend on the region or layer, but they are assumed constant within each layer.

The unknown coefficients used to describe the displacement U are determined from the various conditions. The displacement must be bounded, so $a_1 = 0$; and it must be continuous, so

$$a_2 = (b_1 - b_2)r_1^2 \qquad \text{and} \qquad a_3 = a_2 + (b_2 - b_3)r_2^2, \tag{29}$$

where r_1, r_2, and r_3 denote the radius of the fiber, the primary, and the secondary, respectively. The radial stress component σ_{rr} must be continuous, so

$$b_1(2\lambda_1 + 2G_1) + C\lambda_1 - \beta_1 T$$
$$= b_2(2\lambda_2 + 2G_2) - a_2 2G_2/r_1^2 + C\lambda_2 - \beta_2 T$$
$$b_2(2\lambda_2 + 2G_2) - a_2 2G_2/r_2^2 + C\lambda_2 - \beta_2 T$$
$$= b_3(2\lambda_3 + 2G_2) - a_3 2G_3/r_2^2 + C\lambda_3 - \beta_3 T$$
$$b_3(2\lambda_3 + 2G_2) - a_3 2G_3/r_3^2 + C\lambda_3 - \beta_3 T = 0. \quad (30)$$

Finally, the total longitudinal force or integrated stress must be 0; hence,

$$\frac{1}{2}[r_1^2\sigma_{zz}^{(1)} + (r_2^2 - r_1^2)\sigma_{zz}^{(2)} + (r_3^2 - r_2^2)\sigma_{zz}^{(3)}] = 0 \quad (31)$$

or

$$r_1^2[b_1 2\lambda_1 + C(\lambda_1 + 2G_1) - \beta_1 T]$$
$$+ (r_2^2 - r_1^2)[b_2 2\lambda_2 + C(\lambda_2 + 2G_2) - \beta_2 T]$$
$$+ (r_3^2 - r_2^2)[b_2 2\lambda_3 + C(\lambda_3 + 2G_3) - \beta_3 T] = 0. \quad (32)$$

As for the moments, they are automatically 0 when the coatings are concentric.

These six linear equations in the six unknowns (a_2, a_3, b_1, b_2, b_3, C) can be solved by standard numerical methods. The object of the calculation is the coefficient C, which denotes the thermal strain of the structure. When T is set to 1, then C is α_e, the effective expansion coefficient.

APPENDIX B

Calculation of Spring Constant

This appendix gives a method for calculating the spring constant κ of a fiber within a dual coating. The calculation goes beyond the formula of Vangheluwe[13] by accounting for the elasticity of the outer secondary coating.

Define cylindrical coordinates (r, θ, z) based at the fiber center. The displacement function

$$U = \begin{pmatrix} U_r \\ U_\theta \end{pmatrix}$$

must satisfy the Cauchy Navier equation[15]

$$\nabla^2 U + C\nabla(\nabla \cdot U) = 0 \qquad C = \frac{1}{1 - 2\nu}. \quad (33)$$

The outer surface of the secondary is assumed fixed, and when the rigid fiber is translated δ in the x direction,

$$\delta a_x = \delta(\cos\theta\ a_r - \sin\theta\ a_\theta), \tag{34}$$

the displacement at $r = r_1$ for small δ is

$$U = \begin{pmatrix} \delta \cos\theta \\ -\delta \sin\theta \end{pmatrix}. \tag{35}$$

This means that the angular dependence, in general, is

$$U = \begin{pmatrix} U_r(r) \cos\theta \\ U_\theta(r) \sin\theta \end{pmatrix}. \tag{36}$$

The four solutions of the Cauchy Navier eq. (33) having this angular dependence are

$$\begin{pmatrix} U_r(r) \\ U_\theta(r) \end{pmatrix} = \begin{pmatrix} \ln r/r_1 - \dfrac{C}{2+C} \\ -\ln r/r_1 \end{pmatrix}, \begin{pmatrix} (2-C)r^2 \\ (2+3C)r^2 \end{pmatrix}, \begin{pmatrix} 1 \\ -1 \end{pmatrix}, \begin{pmatrix} r^{-2} \\ r^{-2} \end{pmatrix}, \tag{37}$$

as can be checked by direct substitution. The general solution is a linear combination of these four with four unknown coefficients for each of the two coating layers.

The total of eight unknown coefficients are determined by eight conditions. At r_1,

$$\begin{pmatrix} U_r \\ U_\theta \end{pmatrix} = \delta \begin{pmatrix} 1 \\ -1 \end{pmatrix};$$

at r_3,

$$\begin{pmatrix} U_r \\ U_\theta \end{pmatrix} = \begin{pmatrix} 0 \\ 0 \end{pmatrix};$$

and at r_2,

$$\begin{pmatrix} U_r \\ U_\theta \end{pmatrix}$$

are continuous across the interface. These give six equations. The other two conditions involve the normal stress components σ_{rr} and $\tau_r\theta$, which must be continuous at r_2. In terms of U these are

$$\sigma_{rr} = \lambda \nabla \cdot U + 2\mu \frac{\partial U_r}{\partial r} = (\lambda + 2\mu) \frac{\partial U_r}{\partial r} + \lambda \frac{U_r + U_\theta}{r}$$

$$\tau_r\theta = \mu \frac{\partial U_\theta}{\partial r} - \mu \frac{U_r + U_\theta}{r}, \tag{38}$$

where $\lambda = 2\mu\nu C$ and the angular dependence of eq. (36) has been used. The eight linear equations in eight unknowns can be solved by standard numerical methods.

The force on the fiber for the deflection δ is

$$F = \int_{\text{Fiber}} \sigma \cdot a_x ds = \int_0^{2\pi} (\sigma_r \cos^2\theta - \tau_{r\theta} \sin^2\theta) r_1 d\theta$$

$$= \pi r_1 (\sigma_r(r_1) - \tau_{r\theta}(r_1)). \tag{39}$$

The stress quantity

$$\sigma_r - \tau_{r\theta} = (\lambda + 2\mu) \frac{\partial U_r}{\partial r} - \mu \frac{\partial U_\theta}{\partial r} + (\lambda + \mu) \frac{U_r + U_\theta}{r} \tag{40}$$

equals

$$\left[(\lambda + \mu) \frac{2}{2 + C} + 2\mu \right] 1/r$$

for the first solution in eq. (37) and is identically 0 for the other three. Therefore, when δ is set to 1,

$$\kappa = \pi \left[(\lambda_p + \mu_p) \frac{2}{2 + C_p} + 2\mu_p \right] a_1, \tag{41}$$

where p signifies the primary region and a_1 denotes the coefficient of the first solution,

$$\begin{pmatrix} \ln r/r_1 - \dfrac{C}{2 + C} \\ - \ln r/r_1 \end{pmatrix}$$

in eq. (37), in the primary region. Thus, of the eight unknown coefficients, only one is needed for getting the spring constant.

AUTHOR

Terrence A. Lenahan, S.B. and S.M. (Electrical Engineering), 1964, The Massachusetts Institute of Technology; Ph.D. (Applied Mathematics), 1970, University of Pennsylvania; AT&T Bell Laboratories, 1970—. Mr. Lenahan has done studies in various areas of mathematical physics, including electromagnetic propagation, elasticity, and fluid mechanics. He recently has been interested in mechanical and optical aspects of optical fibers. Member, AAS, AMS, SIAM, AAAS.